HHS Public Access

Author manuscript

J Mol Med (Berl). Author manuscript; available in PMC 2022 March 29.

Published in final edited form as:

J Mol Med (Berl). 2019 December ; 97(12): 1669–1684. doi:10.1007/s00109-019-01853-2.

Keratinocyte-specific ablation of Mcpip1 impairs skin integrity and promotes local and systemic inflammation

Piotr Konieczny[1], **Agata Lichawska-Cieslar**[1], **Patrycja Kwiecinska**[2], **Joanna Cichy**[2], **Roza Pietrzycka**[1], **Weronika Szukala**[1], **Wim Declercq**[3,4], **Michael Devos**[3,4], **Agnieszka Paziewska**[5], **Izabela Rumienczyk**[5], **Maria Kulecka**[5], **Michal Mikula**[6], **Mingui Fu**[7], **Julia Borowczyk**[8,9], **Luis F Santamaria-Babí**[10], **Jolanta Jura**[1]

[1]Department of General Biochemistry, Faculty of Biochemistry, Biophysics and Biotechnology, Jagiellonian University, Gronostajowa 7, 30-387 Krakow, Poland

[2]Department of Immunology, Faculty of Biochemistry, Biophysics and Biotechnology, Jagiellonian University, Gronostajowa 7, 30-387 Krakow, Poland

[3]Molecular Signaling and Cell Death Unit, VIB Center for Inflammation Research Center, Ghent, Belgium

[4]Department of Biomedical Molecular Biology, Ghent University, Technologiepark 71, 9052 Ghent, Belgium

[5]Department of Gastroenterology, Hepatology and Clinical Oncology, Medical Center for Postgraduate Education, Marymoncka 99/103, 01-813 Warsaw, Poland

[6]Department of Genetics, Maria Sklodowska-Curie Memorial Cancer Center and Institute of Oncology, Roentgena 5, 02-781 Warsaw, Poland

[7]Department of Biomedical Science and Shock/Trauma Research Center, School of Medicine, University of Missouri-Kansas City, 5100 Rockhill Rd, Kansas City, MO 64110, USA

[8]Department of Cell Biology, Faculty of Biochemistry, Biophysics and Biotechnology, Jagiellonian University, Gronostajowa 7, 30-387 Krakow, Poland

[9]Current address: Department of Pathology and Immunology, Faculty of Medicine, University of Geneva, Rue Gabrielle Perret-Gentil 4, 1211 Geneva, Switzerland

Jolanta Jura, jolanta.jura@uj.edu.pl.

Piotr Konieczny and Agata Lichawska-Cieslar contributed equally to this work.

Author contributions P.K. and A.L.-C. designed and performed the experiments, and analyzed the data. P.K. performed all the animal work and histological analyses. A.P., I.R., M.K., and M.M. performed RNA sequencing. P.Kw. and J.C performed and analyzed flow cytometry data. R.P., W.S., and J.B. helped with the experiments.W.D.,M.D., and L.S.-B. contributed to data interpretation. M.F. contributed mice. A.L.-C. drafted the main manuscript text; P.K. and J.J. edited it. J.J. coordinated and supervised the project. All authors reviewed the final version of the manuscript

Compliance with ethical standards

Conflict of interests The authors state no conflict of interests.

Declaration of ethics approval These experiments are performed according to law of EU.

Electronic supplementary material The online version of this article (https://doi.org/10.1007/s00109-019-01853-2) contains supplementary material, which is available to authorized users.

[10]Translational Immunology, Department of Cellular Biology, Physiology and Immunology, Faculty of Biology, University de Barcelona, Gran Via de les Corts Catalanes 585, 08007 Barcelona, Spain

Abstract

MCPIP1 (Regnase-1, encoded by the *ZC3H12A* gene) regulates the mRNA stability of several inflammatory cytokines. Due to the critical role of this RNA endonuclease in the suppression of inflammation, Mcpip1 deficiency in mice leads to the development of postnatal multiorgan inflammation and premature death. Here, we generated mice with conditional deletion of Mcpip1 in the epidermis ($Mcpip1^{EKO}$). Mcpip1 loss in keratinocytes resulted in the upregulated expression of transcripts encoding factors related to inflammation and keratinocyte differentiation, such as IL-36α/γ cytokines, S100a8/a9 antibacterial peptides, and Sprr2d/2h proteins. Upon aging, the $Mcpip1^{EKO}$ mice showed impaired skin integrity that led to the progressive development of spontaneous skin pathology and systemic inflammation. Furthermore, we found that the lack of epidermal Mcpip1 expression impaired the balance of keratinocyte proliferation and differentiation. Overall, we provide evidence that keratinocyte-specific Mcpip1 activity is crucial for the maintenance of skin integrity as well as for the prevention of excessive local and systemic inflammation.

Keywords

MCPIP1; Regnase-1; ZC3H12A; Skin inflammation

Introduction

The skin is the main interface between the body and the environment. It is essential for preventing water and electrolyte loss, as well as for protection against harmful substances and pathogens [1]. The impairment of skin barrier function can cause or aggravate skin disorders, including psoriasis, atopic dermatitis, and ichthyosis [2–5]. Although the epidermis is a highly organized stratified epithelium consisting of four distinct layers: stratum basale, stratum spinosum, stratum granulosum, and the uppermost stratum corneum, its barrier function is provided mainly by a number of factors in the stratum corneum (corneocytes), such as lipids, antibacterial peptides, proteases, transcription factors, and many others [6–8]. The unique crosstalk between epidermal layers, immune cells, and microbes is important for tissue repair and regeneration to maintain the skin barrier function [9].

Monocyte chemotactic protein-1-induced protein 1 (MCPIP1), also known as Regnase-1, is encoded by the *ZC3H12A* gene. MCPIP1 possesses a PIN domain that has RNase properties and selectively promotes the destabilization of mRNAs encoding certain inflammatory cytokines, signal transducers, and transcription factors, such as IL-6 and IL12p40 in macrophages and c-Rel, Ox40, and IL-2 in T cells [10–15]. *ZC3H12A* expression is induced by a number of proinflammatory factors, including IL-17A and IL-36 family members [16–18], and MCPIP1 is an essential regulator of inflammatory signaling activation and immune homeostasis [19–22].

The systemic role of MCPIP1 has been demonstrated in Mcpip1-knockout mice. Mice lacking functional Mcpip1 develop postnatal systemic inflammation, which manifests as splenomegaly, lymphadenopathy, abnormal responses of both innate and adaptive immune cells, enhanced cytokine production, and premature death. The lack of Mcpip1 in T cells leads to a similar phenotype, suggesting a key role of Mcpip1 in immune homeostasis [13, 21, 23, 24].

MCPIP1 RNase is upregulated at both the transcript and protein levels in the human psoriatic epidermis [16, 17, 25]. Recent studies have shown that Mcpip1 deficiency leads to exaggerated psoriasis-like skin inflammation in response to imiquimod in both heterozygous Mcpip1$^{-/+}$ mice [16] and in mice with keratinocytespecific Mcpip1 depletion [17]. Importantly, Mcpip1$^{-/+}$ mice do not show any signs of skin pathology at the basal level. Takaishi et al. further pointed out that IL-36 signaling plays a role in driving the development of psoriasiform inflammation in mice with ablated epidermal Mcpip1 function. The authors showed that the expression of some transcripts associated with skin inflammation, such as *Il36a*, *S100a8*, and *Defb3*, is upregulated specifically in Mcpip1-depleted keratinocytes, suggesting that Mcpip1 RNase may play a role in the regulation of keratinocyte biology [18]. However, no description of the in vivo effect of the loss of epidermal Mcpip1 function was provided; in particular, no baseline skin characteristics in the mice were reported [18], which is important to fully understand an impact of Mcpip1 on cutaneous pathophysiology.

To deepen our knowledge on the role of epidermal Mcpip1 in skin homeostasis, we generated keratinocyte-specific Mcpip1-knockout mice (Mcpip1^{EKO}). Based on pathological, immunological, and transcriptional analyses, we found that loss of Mcpip1 function leads to an increase in epidermal thickness as a result of enhanced cell proliferation, skin lesion formation as a result of skin barrier impairment, and spontaneous skin inflammation development due to changes in the expression profile of some inflammatory mediators. Moreover, we found that conditional Mcpip1-knockout mice develop systemic inflammation.

Overall, we provide evidence that Mcpip1 is a novel factor that controls the transcriptional profile in keratinocytes, and is crucial for skin immunological functions and maintaining epidermal homeostasis via the regulation of the equilibrium between keratinocyte proliferation and differentiation. Moreover, we show that Mcpip1 expression positively correlates with the differentiation potential of keratinocytes and postulate that Mcpip1 is a novel factor in the squamous epidermis that is essential for the maintenance of skin integrity.

Materials and methods

Animals

The Cre-loxP system was used to generate Mcpip1^{EKO} mice (C57BL/6NJ). The Mcpip1$^{loxP/loxP}$ (Mcpip1$^{fl/fl}$) mice, herein control mice, have been described previously [26]. To generate Krt14^{Cre}Mcpip1$^{fl/fl}$ mice, male Krt14^{Cre} mice [27] were bred with female Mcpip1 loxP-flanked mice. The mice used in this study were sex- and age-matched littermates. All animal procedures were conducted in accordance with the Guide for the

Care and Use of Laboratory Animals (Directive 2010/63/EU of the European Parliament) and carried out under a license from the Ethical Committee of Jagiellonian University.

Human primary keratinocyte differentiation

Normal human epidermal keratinocytes were obtained from Lonza Group Ltd. (Basel, Switzerland). The cells were cultured in a 75-cm^2 cell-culture flask at 37 °C in a 5% CO_2 atmosphere in serum-free Keratinocytes Growth Medium KGM-Gold (Lonza Group Ltd., Basel, Switzerland) supplemented with bovine pituitary extract, human endothelial growth factor, bovine insulin, hydrocortisone, gentamicinamphotericin B (GA-1000), epinephrine, and transferrin. To promote differentiation, primary keratinocytes were cultured in 6-well plates with serum-free keratinocyte growth medium KGM-Gold supplemented with 1.8 mM calcium.

Primary keratinocyte isolation

Mouse primary keratinocytes were isolated from newborn (0– 1 days) control ($Mcpip1^{fl/fl}$) or Mcpip1-deficient ($Krt14^{Cre}Mcpip1^{fl/fl}$) pups. The newborn mice were killed by decapitation and incubated for 1 min in PBS (Lonza, MD, USA), 1 min in 70% EtOH, and 1 min in PBS with antibiotics (Lonza, MD, USA). To separate the epidermis from the dermis, the skin was cut into small pieces and incubated with 2 mL of dispase (StemCell Technologies, MA, USA) overnight at 4 °C. The next day, the skin was transferred into a 6-cm dish, and the epidermis was separated from the dermis with forceps. Epidermal sheets were incubated in 1 mL of 0.25% trypsin with EDTA for 15 min at room temperature (RT). Keratinocytes were washed out of the epidermal sheet using 5 mL of DMEM (Lonza, MD, USA) supplemented with 10% fetal bovine serum (FBS, Sigma-Aldrich). After centrifugation, keratinocytes were seeded in cell-culture plates in 10% FBS/DMEM. After 24 h, the medium was replaced with keratinocyte growth medium (keratinocyte cell basal medium supplemented with KGM-Gold™ SingleQuots™ (bovine pituitary extract, human endothelial growth factor, insulin (bovine), hydrocortisone, gentamicin-amphotericin B (GA-1000), epinephrine, and transferrin); Lonza, MD, USA). Keratinocytes were cultivated at 37 °C with 5% CO_2, and the medium was refreshed every 2 days.

RNA isolation and quantitative real-time PCR

Skin samples or spleens were collected, placed in Eppendorf tubes, frozen in liquid nitrogen, and stored at − 80 °C. For RNA isolation, the samples were homogenized in Fenozol (A&A Biotechnology, Gdynia, Poland) using a tissue homogenizer (Miccra D-1, Germany). The quantity of ribosomal RNA and DNA contaminants was examined using electrophoresis in a 1% denaturing formaldehyde gel. The purity and concentration of total RNA were assessed using a NanoDrop 1000 spectrophotometer (Thermo Fisher Scientific, Waltham, MA, USA). Reverse transcription was performed with 1 μg of total RNA, oligo(dT) primer, and M-MLV reverse transcriptase (Promega, Madison, USA). The cDNA was diluted 5 times, and real-time PCR was performed using an Eco Real-Time PCR System (Illumina) with SYBR Green qPCR master mix (A&A Biotechnology). The relative abundance of transcripts was determined compared to the abundance of elongation factor-2 (EF2). The sequences of the primers (Sigma-Aldrich) are listed in Supplementary Table S1

RNA sequencing

RNA extraction—Total RNAwas extracted from mouse primary keratinocytes using a mirVana™ PARIS™ kit (Ambion) according to the manufacturer's instructions. The concentration of each sample was measured using a NanoDrop 2000 spectrophotometer (Thermo Fisher Scientific). The total RNA quality was analyzed with a RNA 6000 Nano Kit on an Agilent 2100 bioanalyzer (Agilent). Only samples with an RNA integrity number (RIN) > 7 were considered for downstream analyses.

Mouse AmpliSeq transcriptome—An Ion AmpliSeq Transcriptome Mouse Gene Expression kit (Thermo Fisher Scientific) was used for library preparation from IMQ-treated samples according to the manufacturer's protocol. Briefly, 100 ng of total RNA was reverse transcribed, and the cDNA was subjected to multiplex PCR to amplify fragments of the target transcripts. The amplicons were then subjected to partial digestion at the primer sequences followed by adaptor ligation to the amplicons and purification on magnetic beads. The generated library was quantified on a 2100 Bioanalyzer using a DNA 1000 kit (Agilent).

Sequencing on an Ion Proton System—Each library was diluted to ~ 80 pM prior to template preparation. Eight barcoded libraries were mixed at equal volumes and used for automatic template preparation on an Ion Chef (Thermo Fisher Scientific) instrument using reagents from an Ion PI Hi-Q 200 Kit (Thermo Fisher Scientific) and Ion PI v3 Proton Chip. The samples were sequenced on the Ion Proton System (Thermo Fisher Scientific) according to the manufacturer's instructions.

Gene expression analysis—Gene abundance was quantified with htseq-count (HTSeq framework version 0.6) [28] using Ensembl Gene gtf files from UCSC as a reference. Differential gene expression was analyzed with the R package DESeq2, version 1.10.1. The sequencing data (as mapped bam files) are available in the European Nucleotide Archive under accession number PRJEB31970.

Gene Ontology category analysis—Gene function annotation was performed using the Database for Annotation, Visualization, and Integrated Discovery v.6.8 (DAVID v.6.8). Gene Ontology Biological Processes (GO_BP) analyses were used to achieve functional annotation-based clustering of genes with upregulated and downregulated expression [29, 30].

Protein isolation and Western blotting

For protein isolation, skin or spleen samples were homogenized in RIPA buffer supplemented with a complete protease inhibitor cocktail (Roche, Basely, Switzerland) and a PhosSTOP phosphatase inhibitor cocktail (Roche) using a tissue homogenizer (Miccra D-1, Germany). Cultured keratinocytes were washed with PBS and lysed in RIPA buffer supplemented with protease and phosphatase inhibitors. The protein concentrations in the cell lysates were measured with the bicinchoninic acid assay. Tissue and cell lysates were separated by SDS/PAGE on 10% polyacrylamide gels and electrotransferred to PVDF membranes (Millipore, Billerica, MA, USA), which were blocked in 3% milk dissolved in Trisbuffered saline containing 0.05% Tween 20 (BioShop, Burlington, Canada). The

membranes were incubated with primary antibodies overnight at 4 °C. Then, the membranes were incubated with horseradish peroxidase (HRP)-conjugated secondary antibodies. The signal was detected using Immobilon Western Chemiluminescent HRP Substrate (Millipore) in a MicroChemi chemiluminescence detector (DNR Bio-Imaging Systems, Jerusalem, Israel). The antibodies used in this study are listed in Supplementary Table S2.

Histology and immunofluorescence staining

Skin tissue specimens were fixed in 4% formaldehyde for 2 h and then incubated overnight at 4 °C in 30% sucrose. The next day, the tissue samples were embedded in Tissue-Tek O.C.T. Compound (Fisher Scientific, Pittsburgh, PA, USA). Subsequently, 6–8-μm cryosections were cut and stained with hematoxylin and eosin (H&E). Antigen retrieval was performed in 10 mM citrate buffer (pH 6.0) for 30 min at 95 °C. For immunohistology, skin samples were stained using an EnVision G|2 System/AP, Rabbit/Mouse (Permanent Red) kit (Dako, Glostrup, Denmark) according to the manufacturer's protocol. After staining, the skin samples were counterstained with Mayer's hematoxylin, mounted in glycerol mounting medium (Dako), and examined with a Leica CTR6 LED. For immunofluorescence, nonspecific antibody binding was prevented by blocking with 5% horse/goat serum, 1% BSA, and 0.005% Tween (Sigma-Aldrich) in PBS for 1 h. Primary antibodies were incubated overnight at 4 °C in blocking buffer. The sections were rinsed in PBS and incubated with secondary antibodies for 1 h at room temperature. Nuclei were stained with Hoechst 33258 (Sigma-Aldrich). Samples were mounted with fluorescent mounting medium (Dako) and then examined with a Leica CTR6 LED (Leica Microsystems, Wetzlar, Germany) equipped with Lecia Application Suite X software. The antibodies utilized for staining are listed in Supplementary Table S2. Figures were prepared using ImageJ and Adobe Illustrator CC.

Barrier function assay

An in situ skin permeability assay using toluidine blue was performed as previously described [31]. Briefly, newborn mice were sacrificed and incubated in methanol/PBS (25, 50, 75, and 100%) for 1 min and then thoroughly washed with PBS. Pups were subsequently immersed in 0.0125% toluidine blue/PBS for 1 min. Destaining was performed with PBS washing before photographs were captured. Transepidermal water loss (TEWL) measurements were performed on adult mice (3 months old (mo)) using a Tewameter TM300 (Courage + Khazaka Electronic) according to the manufacturer's operating instructions. Adult mice were dorsally shaved using a professional hair clipper. Twenty-four hours later, mice were anesthetized and after 10 min the measurements were taken. Data were expressed in g/m^2h.

Flow cytometry

Blood samples were collected by retro-orbital bleeding into tubes containing 10 mM EDTA. Bone marrow cells were isolated from one femur by flushing with RPMI1640 medium (Biowest) supplemented with 2% FBS (Gibco). Then, $0.5cm^2$ back skin samples were cut into small pieces and incubated with 2.5 mg/mL Collagenase D (Roche Diagnostics) solution at 37 °C with continuous shaking at 1400 rpm for 45 min. Single-cell suspensions from the skin, spleen, and bone marrow were obtained by mashing the organs through

40-μm cell strainers in RPMI1640 medium (Biowest) supplemented with 2% FBS (Gibco). After the removal of red blood cells by treatment with lysis buffer (155 mM NH_4Cl, 10 mM $NaHCO_3$, 0.1 mM EDTA), the cells were washed in PBS and then stained for viability assessment (Zombie Aqua Fixable Viability Kit; BioLegend). After being washed, the cells were blocked with anti-CD16/CD32 antibodies (Fc block; eBioscience) for 10 min on ice. Then, the cells were stained with the appropriate directly conjugated antibodies listed in Supplementary Table S2 and then washed with PBS containing 1% BSA. Data were acquired on a BD LSRII (BD Biosciences). Singlets were selected based on FCS-A vs FCS-H. Dead cells were routinely excluded from the analysis. “Fluorescence minus one” (FMO) controls were routinely used to verify correct compensation and to set the thresholds for positive/negative events. Analyses were performed with FCS Express (De Novo Software).

Quantification and statistics

All analyses were performed with 3–11 independent biological replicates. GraphPad Prism 7 (GraphPad Software Inc., La Jolla, CA) was used for all analyses of numerical data and the generation of graphs and statistical tests, including one-way analysis of variance (ANOVA) and Student’s *t* test. Error bars represent the standard error of the mean.

Results

Mcpip1 RNase regulates the transcript level of immune response and terminal differentiation genes in keratinocytes

Epidermal keratinocytes undergo a multistep differentiation process that requires a tight balance between their proliferation and differentiation. To investigate the involvement of the MCPIP1 protein in this process, we characterized its expression in normal human keratinocytes and found that its expression is upregulated during Ca^{2+}-induced differentiation in vitro, concurrently with that of keratin 10, a marker of epithelial differentiation (Fig. 1a, b). This finding is consistent with the observation that MCPIP1 protein localizes predominantly in the differentiated suprabasal layers of the normal human epidermis [17].

To determine the role of Mcpip1 in epidermal physiology in vivo, we generated $Krt14^{Cre}Mcpip1^{fl/fl}$ ($Mcpip1^{EKO}$) mice, in which Mcpip1 is specifically deleted in epidermal keratinocytes (Fig. 1c). Cre-mediated recombination resulted in the complete elimination of Mcpip1 mRNA and protein expression in primary keratinocytes (Fig. 1d and Supplementary Fig. S1). The $Mcpip1^{EKO}$ pups were born viable with a consistent body weight reduction of approximately 10% (Fig. 1e, f) but did not exhibit any obvious phenotypic abnormalities, including an intact outside-in stratum corneum barrier (Fig. 1g).

In the subsequent experiments, we performed a thorough biochemical and/or immunological characterization of $Mcpip1^{EKO}$ mice at three developmental stages: newborn (P0), adult (3 mo), and old (6–8 mo; Fig. 1h). We began the analysis by comparing the transcriptomes of keratinocytes isolated and cultured from the newborn control and $Mcpip1^{EKO}$ mice by RNA sequencing (RNA-Seq). The pairwise gene comparison indicated that the expression of 392 and 207 transcripts was significantly up- or downregulated (adj. *P* value < 0.05

and fold change > 1.5), respectively, in Mcpip1^{EKO} cells. Functional analysis by Gene Ontology (GO) enrichment annotation revealed that the genes with upregulated expression in Mcpip1^{EKO} mice were mainly assigned to groups related to keratinocyte differentiation and inflammatory responses (Fig. 2a, b). The expression of keratin (*Krt6b*, *Krt16*, and *Krt23*) and small proline-rich protein 2 (*Sprr2d/e/h*) family genes associated with epidermal growth, inflammation, and differentiation was enhanced in Mcpip1-deficient cells. The upregulated expression of interleukin-36α (IL-36α; *Il36a/Il1f6*) and IL-36γ (*Il36g/Il1f9*) cytokines, S100a8/a9 antibacterial peptides, and lipocalin-2 (*Lcn2*) indicated persistent proinflammatory signaling in Mcpip1^{EKO} cells. Our RNASeq data are consistent with the known functions of MCPIP1 RNase as a negative regulator of immune responses. However, we also noticed the elevated expression of certain negative regulators of inflammation, such as *Il1rn* and *Il36ra/Il1f5* transcripts that encode IL-1 and IL-36 receptor antagonists (Fig. 2a, c). Other pathways found to be elevated in Mcpip1^{EKO} keratinocytes were related to lipid metabolism, oxidation-reduction processes, and apoptosis (Fig. 2a, b). Among the genes with upregulated expression that are important regulators of lipid metabolism processes are arachidonate 12-lipoxygenase, 12S type (*Alox12*), lipase, family member K (*Lipk4*), and fatty acid-binding protein 5 (*Fabp5*). Examples of transcripts encoding positive regulators of cell death shortlisted in our RNA-Seq data include TNF receptor superfamily member 6 (*Fas*), bone morphogenetic protein (*Bmp4*), and hypoxia-inducible factor 3-alpha (*Hif3a*).

Newborn Mcpip1^{EKO} mice exhibit disturbances in the distribution of the epidermal keratins Krt10/Krt14, Krt6, and PCNA

We next investigated the in vivo effects caused by the loss of keratinocyte Mcpip1 function. Histological analyses showed that the epidermis of newborn Mcpip1^{EKO} mice was 1.2-fold thicker than those of control mice (Fig. 3a, b), suggesting alterations in epidermal proliferation and/or differentiation. QRT-PCR analyses of keratinocyte differentiation-associated markers indicated that the basal expression of involucrin (*Ivl*) and keratin 10 (*Krt10*) in the Mcpip1^{EKO} neonatal epidermis was unchanged (Fig. 3c). In contrast, Mcpip1 loss resulted in the marked increase in *Sprr2d*, *Krt6a*, *Krt6b*, and *Krt16* transcripts (Fig. 3d), suggesting an abnormal keratinocyte differentiation program in the Mcpip1^{EKO} mouse epidermis. Subsequently, we analyzed the expression of several differentiation- and proliferation-specific markers by immunofluorescence. We found that there were occasionally keratin 10/keratin 14 (Krt10/Krt14) double-positive cells in suprabasal layers of Mcpip1-deficient epidermis, indicating the coexpression of basal and spinous keratins (Fig. 3e). The suprabasal expansion of Krt14 may be the result of a mild increase in inflammatory signaling within the Mcpip1^{EKO} mouse epidermis. We further analyzed the protein expression of keratin 6 (Krt6). Under homeostatic conditions, in normal neonatal epidermis, Krt6 expression is restricted to the hair follicles. In response to biochemical or mechanical stress, under hyperproliferative conditions or due to keratinocyte differentiation defects, Krt6 expression is induced in the interfollicular epidermis [32–36]. Interestingly, we observed intermittent expression of Krt6 in the interfollicular epidermis of the Mcpip1^{EKO} neonates, whereas in the control neonates, its expression was restricted to the hair follicles. This observation is consistent with our QRT-PCR data, which indicated increased levels of *Krt6* mRNA in transgenic neonatal skin lysates. The induction of Krt6 expression in the suprabasal epidermis is a further indication of altered epidermal differentiation in

Mcpip1^{EKO} mice. In addition to the abnormalities in keratin expression, we observed a 1.3-fold increase in the abundance of epidermal proliferating cell nuclear antigen (PCNA)-positive cells, indicating the increased proliferation of Mcpip1^{EKO} basal keratinocytes in vivo (Fig. 3f, g).

Increased expression of proinflammatory factors in newborn and young Mcpip1^{EKO} mouse skin coincides with an impairment of skin integrity and the development of signs of systemic inflammation

We next carried out QRT-PCR expression analyses of the most significantly altered inflammation-related genes detected preliminarily in the Mcpip1^{EKO} keratinocytes in the whole skin of both newborn (P0) and young mice (3 mo). We found that the levels of *Il36a/g* and *S100a8/a9* were significantly elevated within Mcpip1^{EKO} skin (Fig. 4a), consistent with our in vitro data (Fig. 2c). For instance, Il36a expression was increased in the P0 and 3-month-old Mcpip1^{EKO} skin by ~ 5- and ~ 10-fold, respectively (Fig. 4a). The lack of epidermal Mcpip1 led to increased levels of other proinflammatory mediators in the skin. Notably, the mRNA expression of *Tnfa*, a cytokine associated with Th1 response, was increased in both newborn (P0) and young (3 mo) Mcpip1^{EKO} skin (Fig. 4b). The expression of *Il6* was ~ 3-fold elevated in Mcpip1^{EKO} compared to the control (P0) pups, but its levels were not significantly altered in the skin of young (3 mo) mice (Fig. 4b). In contrast, the expression of *Il18* mRNA was unchanged in the newborn (P0) mice and increased slightly in the young (3 mo) mice (Fig. 4b).

In newborn mice (P0), we also noticed the differential expression of transcripts encoding the cytokine IL-33 that exerts both pro- and anti-inflammatory effects [37]. In the Mcpip1^{EKO} skin (P0), the Il33 mRNA levels were increased ~ 2.5-fold (Fig. 4b). We next assayed whether elevated inflammatory signaling within the Mcpip1^{EKO} mouse skin is reflected in the phenotype of skin immune cells. Flow cytometry analyses of 3-month-old mouse back skin homogenates indicated excessive presence of eosinophils in the Mcpip1^{EKO} dermis (Fig. 4c). There were no significant changes in the relative frequencies of other leukocytes, including neutrophils, monocytes, macrophages, and T lymphocytes (Supplementary Fig. S2a). Cutaneous B cells were barely detected in both the Mcpip1^{EKO} and control mice (data not shown).

To determine whether elevated levels of inflammatory mediators are associated with changes in skin barrier integrity in Mcpip1^{EKO} mice, we measured TEWL. The TEWL was analyzed in the 3-month-old mice showing no macroscopic signs of skin inflammation. The Mcpip1^{EKO} mice demonstrated significantly (1.5-fold) higher TEWL rates than control mice, suggesting reduced skin barrier function (Fig. 4d).

Despite molecular, immunological, and skin barrier function defects, the skin of 3-month-old Mcpip1^{EKO} mice did not show any phenotypic signs of skin pathology. We also did not observe alterations in body weight (Supplementary Fig. S2b). However, young Mcpip1^{EKO} mice showed a mild systemic effect, as evidenced by the enlarged lymph nodes and spleens (Fig. 4e), which were 1.4-fold heavier than those of the control (Fig. 4f). The flow cytometry analysis of splenic and blood CD45+ cells did not yet show any significant differences between the control and Mcpip1^{EKO} mice (Fig. 4g and Supplementary Fig. 2c). However, in

the bone marrow, statistically significant increase and decrease in population of eosinophils and B cells, respectively, was observed (Fig. 4h).

Old Mcpip1^{EKO} mice have aggravated skin and systemic inflammation

Although newborn and young (3 mo) Mcpip1^{EKO} mice did not develop a skin inflammation phenotype, aging Mcpip1^{EKO} mice progressively developed skin inflammation. At approximately 4 months of age, the mice started to develop chronic wounds around their cheeks, ears, necks, and trunks, which were accompanied by hair loss within the affected areas (Fig. 5a, b). Adult (6 mo) Mcpip1^{EKO} mice exhibited 13% reduced body weight (Fig. 5c), splenomegaly, and enlarged lymph nodes (Fig. 5d). The spleens of old Mcpip1^{EKO} mice were 2.2-fold heavier than those of control mice (Fig. 5e). Flow cytometric analyses showed a significant increase in neutrophil (~ 4-fold), eosinophil (~ 8-fold), monocyte (2.4-fold), and macrophage (2.1-fold) numbers in Mcpip1^{EKO} old mice compared to control mice, but a decreased presence of the B and T lymphocytes among splenocytes (Fig. 5f). Together, these data indicate substantial systemic changes in immune compartment of the adult Mcpip1^{EKO} mice. At the histological level, the skin lesions exhibited hyperkeratosis with dysplastic keratinocytes populating the invaginations, which led to a profound increase in the epidermal thickness within the Mcpip1^{EKO} skin lesions (Fig. 5g, h). In addition, compared to the control mice, the aging (6 mo) Mcpip1^{EKO} mice exhibited a profound 2.3-fold reduction in the thickness of the hypodermis within the unaffected skin (Fig. 5i), possibly as a result of the elevated inflammation in Mcpip1^{EKO} mice.

We next characterized the skin pathologies that developed in old mice upon Mcpip1 deletion in detail and found that significant thickening of the Mcpip1^{EKO} lesional epidermis corresponded with altered Krt14/Krt10 expression. We noticed the suprabasal expansion of basal Krt14 expression and reduction in the early differentiation marker Krt10 (Fig. 5j). The hyperproliferative phenotype was further confirmed by staining for the proliferation markers Krt6 and PCNA, which revealed an increase in the number of actively proliferating cells in both basal and suprabasal compartments (Fig. 5k).

Cutaneous inflammatory phenotype of adult Mcpip1^{EKO} mice also manifested in the enhanced production of various proinflammatory factors. In particular, the transcript levels of *Il36a/g*, *Tnfa*, *Il1b*, and *Il6* cytokines; *Cxcl2* chemokine; *S100a8/a9* antibacterial peptides; and *Sprr2d* increased profoundly within lesional Mcpip1^{EKO} skin (Fig. 6a). We also noticed a significant increase in the *Il33* transcript level, as well as elevated matrix metallopeptidase 9 (Mmp9) and arginase-1 (Arg1; Fig. 6a). The activation of proinflammatory factors within the Mcpip1^{EKO} skin lesion was positively correlated with the activation of Stat3 (Fig. 6b–d). In addition, the infiltration of the Mcpip1^{EKO} lesional dermis by macrophages (Fig. 6e), mast cells (Fig. 6f), and neutrophils (Fig. 6g) was observed, suggestive of skin inflammatory phenotype acquired by the Mcpip1^{EKO} mice upon aging.

Discussion

In response to pathogens or other environmental factors, keratinocytes release proinflammatory mediators that attract and stimulate immune cells, initiating an inflammatory response. Therefore, keratinocytes serve as a physical barrier and provide

tight control of inflammatory processes to avoid overreaction and tissue damage. MCPIP1 is an important regulator of inflammatory responses; however, there is also evidence that it is a regulator of proliferation, differentiation, angiogenesis, and cell metabolism [38–41]. To explore the role of MCPIP1 in skin homeostasis, we generated keratinocyte - specific Mcpip1-knockout mice (Mcpip1^{EKO}).

Although newborn and young Mcpip1^{EKO} mice did not exhibit any obvious macroscopic abnormalities, histological analyses indicated epidermal thickening with the presence of Krt14/Krt10 double-positive cells in the suprabasal layers that correlated with the increased proliferation of basal and suprabasal keratinocytes. The perturbed Krt14/Krt10 distribution was reflected in our Mcpip1-depleted keratinocyte RNA-Seq results, in which the levels of transcripts associated with keratinocyte differentiation were increased compared to those in control keratinocytes. For example, the expression of “stress keratins,” *Krt6b* and *Krt16*, which are associated with hyperproliferation and inflammation of the epidermis [42], was enhanced. This observation was confirmed by QRT-PCR analyses of whole skin lysates of newborn Mcpip1^{EKO} pups. Furthermore, immunostaining showed abnormal Krt6 expression in the interfollicular epidermis of Mcpip1^{EKO} pups, most likely due to the elevated inflammatory signaling present in their skin. We also noticed a prominent increase in the transcriptional expression of the terminal differentiation marker Sprr2d in both isolated keratinocytes and newborn mouse skin. Together, these data strongly suggest that there is an imbalance in keratin reprogramming within the Mcpip1^{EKO} epidermis. Significant differences in the profiles of transcripts encoding proinflammatory mediators, such as the IL-36α/γ cytokines, were observed in Mcpip1^{EKO} keratinocytes or in the skin of young mice. Nevertheless, this increase in the levels of inflammatory mediators did not lead to macroscopically visible skin inflammation in young mice, possibly due to the sufficient levels of negative regulators of inflammation, the transcript levels of which were also elevated in Mcpip1^{EKO} keratinocytes. These negative regulators include IL-36/IL-1 receptor antagonists and interleukin-1 receptor-associated kinase (Irak3). The increase in the mRNA levels of IL-36α and of the antimicrobial proteins S100a8, S100a9, and Lcn2 in Mcpip1-depleted keratinocytes is consistent with the results of previous reports [17, 18, 43].

Our comprehensive QRT-PCR analysis of the transcriptional expression of several inflammatory factors in the whole skin of newborn and young (3 mo) mice revealed that the levels of *Il36a*, *Il36g*, *S100a8*, and *S100a9* detected preliminarily in our RNA-Seq analysis were also elevated in the whole skin of newborn and young Mcpip1^{EKO} mice. In addition to the elevated levels of these factors, we noticed elevated transcript levels of *Il6*, *Tnfa*, and *Il33* in the newborn mice and of *Tnfa* and Il18 in the young (3 mo) mice. The elevated expression of a plethora of inflammatory mediators in the Mcpip1^{EKO} skin that are released into the circulation is likely responsible for triggering the development of mild systemic inflammation in young (3 mo) mice, which manifests as the enlargement of the spleen and lymph nodes. To ensure the specificity of our conditional knockout model, we validated that the transcriptional and translational expression of Mcpip1 in the spleens of 3-month-old mice was unaltered (Supplementary Fig. S3a and S3b).

Despite the disturbances observed at the molecular level (elevated expression of inflammatory factors and abnormal epidermal proliferation/differentiation patterns), the skin

of newborn and young (3 mo) Mcpip1^{EKO} mice did not show any overall macroscopic changes. The skin barrier of newborn Mcpip1^{EKO} mice was intact (indicated by the toluidine blue dye penetration assay), whereas the young (3 mo) mice showed impairment of skin barrier function, as indicated by the significantly elevated TEWL level, which most likely was the cause of the progressive development of local and possibly mild systemic inflammatory responses. However, upon aging, Mcpip1^{EKO} mice gradually developed local skin pathologies. As a result of systemic inflammation and impairment of the skin barrier function, 4-month-old mice began to exhibit chronic skin lesions, with noticeable dermal presence of mast cells, neutrophils, and macrophages. The appearance of keratin pearls, which are characteristic of squamous cell carcinoma but can also occur in benign hyperproliferative tissue, indicates an abnormal keratinization pattern in the Mcpip1^{EKO} adult skin and is most likely the result of excessive proliferation. The abnormally high levels of transcripts encoding Sprr2d protein as well as the altered expression of Krt14/ Krt10, Krt6, and PCNA correlated with the perturbed differentiation and proliferation within the Mcpip1^{EKO} skin lesions. It was reported that enhanced levels of the cornified envelope protein Sprr2d lead to corneocyte fragility, resulting in a barrier defect, mild inflammation, and keratinocyte hyperproliferation [44]. The upregulation of Krt6 expression manifested within Mcpip1^{EKO} skin lesions in old mice was associated with the downregulation of Krt10 expression and upregulation of the transcriptional expression of inflammatory factors (e.g., Tnfα, IL-1β, and IL-6) that are generally involved in the activation of stress keratins [45–47]. In addition to their mechanical properties, these keratins have specialized functions upon barrier breach and play important roles in various pathologies. Generally, the induction of Krt6 and Krt16 expression occurs at the expense of the Krt1/Krt10 pair in the postmitotic layers of the interfollicular epidermis under conditions of environmental stress (e.g., tissue injury, UV exposure, and viral infection) and in some diseases (e.g., psoriasis and carcinoma) [32–36]. In addition, the elevated mRNA expression of a plethora of proinflammatory mediators and chemokines, such as IL-1β, IL-6, IL-36α, S100a8/a9, and Cxcl2, within Mcpip1^{EKO} skin lesion, and activation of Stat3, is associated with the enhanced proliferation rate and the exaggeration of the inflammatory response in the skin. The transcriptional expression of *Il18*, which was transiently activated in young Mcpip1^{EKO} mice, was not altered in the old mouse skin (Supplementary Fig. S4a). Similarly, no differences in the expression of *Il23a* were found, suggesting that the Th17 response is not involved in the development of Mcpip1^{EKO} skin lesions (Supplementary Fig. S4a). However, we noticed a prominent increase in the Il33 transcript level in skin lesions. This pleiotropic cytokine acts as an “alarmin” in response to external stimuli or tissue damage. The IL-33/ST2 pathway regulates the balance between extensive inflammation and tissue remodeling [37, 48, 49]. In skin lesions of Mcpip1^{EKO} mice, we also noticed the transcriptional activation of *Mmp9* metallopeptidase expression, most likely enhanced by IL-33 [49, 50]; and of arginase-1, a marker of alternatively activated macrophages, the expression of which increases upon tissue injury and repair [51, 52]. The extracellular matrix proteins of the basement membrane zone (BMZ) are important components of the intrafollicular epidermis (IFE) stem cell niche and functionally connect the dermis and epidermis. Type XVII collagen is expressed in basal keratinocytes and is involved in keratinocyte proliferation and migration [53, 54]. Here, we did not observe significant differences in collagen XVII expression between skin lysates

from old Mcpip1^{EKO} and control mice healthy skin. However, a small reduction in the ectodomain in the Mcpip1^{EKO} skin lesions was observed (Supplementary Fig. S4b and S4c). Collagen XVII undergoes posttranslational modifications, such as ectodomain shedding and degradation, in physiological and pathological settings through the action of several proteases, such as disintegrin and metalloproteinases ADAM9/10/17, MMP9, neutrophil elastase, and other serine proteases [55, 56]. In the Mcpip1^{EKO} mouse skin lesions, we observed the upregulation of *Mmp9* expression and neutrophil infiltration. Our results suggest that ectodomain shedding of collagen XVII may be involved in Mcpip1^{EKO} skin lesion development; however, this observation requires further analysis. In conclusion, we identified the activation of both proand anti-inflammatory signaling pathways in Mcpip1^{EKO} mouse skin lesions; however, the levels of anti-inflammatory factors were not sufficient to resolve the chronic inflammation and promote skin remodeling.

Systematically, as a result of the enhanced skin inflammation, a vast range of proinflammatory factors that were increased in the old (6–8 mo) Mcpip1^{EKO} mouse skin were further released into the circulation and likely exacerbated the systemic inflammation, which phenotypically manifested as enlarged spleens and reduced body weight. We hypothesize that the transcriptional activation of IL-33 observed within the skin lesions of old Mcpip1^{EKO} mice contributes to the activation of the immune system via the ST2 receptor and exaggerates neutrophil- and eosinophil-dominated systemic inflammation [37, 57, 58]. IL-33-overexpressing mice are born with reduced body weight and progressively develop systemic inflammation with neutrophilia and increased myelopoiesis [58]. In a recent study, Peng and co-authors showed that in mice Mcpip1 loss contributes to the development of Th2-associated allergic airway inflammation. It was proposed that Mcpip1 is a negative regulator of Th2 function through the Notch/Gata3 pathway [59]. It would be interesting to evaluate the mechanism that contributes to the inflammatory phenotype of the Mcpip1^{EKO} mice. The systemic, myeloid celldominated inflammatory phenotype observed in old, 6–8 mo, Mcpip1^{EKO} mice suggests that myelopoiesis may be enhanced in Mcpip1^{EKO} mice. This hypothesis is supported by the increased frequencies of myeloid cell populations, including neutrophils, eosinophils, monocytes, and macrophages, and reduced lymphocyte (B and T cells) populations in the spleens of Mcpip1^{EKO} mice. In addition, myeloid cells tend to be more prevalent, whereas lymphocytes less prevalent among leukocytes in the bone marrow of young Mcpip1^{EKO} mice, with significantly increased and decreased frequencies of eosinophils and B cells, respectively, supporting our hypothesis.

The prevalent factor triggering “spontaneous” skin inflammation in Mcpip1^{EKO} mice remains elusive. It would be interesting to investigate whether these mice develop skin lesions in germ-free conditions because it has been shown that antibiotic treatment can improve inflammation and survival in completely Mcpip1-deficient mice [24]. Therefore, Mcpip1^{EKO} mice may respond to the otherwise harmless skin microbiota. Alternatively, these skin lesions could be the consequence of elevated levels of proinflammatory factors in the skin, mild allergic reactions, and progressive systemic inflammation that contribute to itching and the development of mild scratching-induced wounds, the healing of which is impaired by the absence of Mcpip1. The progressive loss of skin integrity can be caused by several factors, including skin dehydration, thinning of the subcutaneous lipid layer, and systemic inflammation.

In conclusion, we postulate that epidermal Mcpip1 is essential for proper keratinocyte differentiation and epidermal functioning. Our study demonstrates a previously undescribed function of Mcpip1, which is required in keratinocytes for their proper differentiation and the maintenance of skin integrity. Our data also indicate that the normal functioning of Mcpip1 in keratinocytes is essential for the maintenance of systemic homeostasis, as the deficiency of this protein in aging mouse keratinocytes results in an inflammatory response that impacts multiple tissues and organs, including adipose tissue and the spleen.

Supplementary Material

Refer to Web version on PubMed Central for supplementary material.

Acknowledgments

For the Krt14^{Cre} mice, we are very thankful to Prof. Carien Niessen (Germany). We are grateful to the staff of the animal facility of the Faculty of Biochemistry, Biophysics and Biotechnology for help with animal breeding.

Funding information This research was supported by grants from the National Science Centre: PRELUDIUM 2014/13/N/NZ3/00729 (to P.K.) and OPUS 2016/23/B/NZ3/00792 (to J.J.). The Faculty of Biochemistry, Biophysics and Biotechnology of Jagiellonian University is a partner of the Leading National Research Centre (KNOW) supported by the Ministry of Science and Higher Education. W.D. was supported by the Flanders Institute for Biotechnology (VIB), a UGent grant (GOA-01G01914) and by Methusalem grant (BO16/MET_V/007, Ghent University).

References

1. Nestle FO, Di Meglio P, Qin J-Z, Nickoloff BJ (2009) Skin immune sentinels in health and disease. Nat Rev Immunol 9:679–691 [PubMed: 19763149]
2. Elias PM, Williams ML, Holleran WM, Jiang YJ, Schmuth M (2008) Pathogenesis of permeability barrier abnormalities in the ichthyoses: inherited disorders of lipid metabolism. J Lipid Res 49:697–714 [PubMed: 18245815]
3. Guttman-Yassky E, Nograles KE, Krueger JG (2011) Contrasting pathogenesis of atopic dermatitis and psoriasis—part I: clinical and pathologic concepts. J Allergy Clin Immunol 127:1110–1118 [PubMed: 21388665]
4. Segre JA (2006) Epidermal barrier formation and recovery in skin disorders. J Clin Invest 116:1150–1158 [PubMed: 16670755]
5. van Smeden J, Bouwstra JA (2016) Stratum corneum lipids: their role for the skin barrier function in healthy subjects and atopic dermatitis patients. Curr Probl Dermatol 49:8–26 [PubMed: 26844894]
6. Elias PM, Gruber R, Crumrine D, Menon G, Williams ML, Wakefield JS, Holleran WM,Uchida Y (1841) Formation and functions of the corneocyte lipid envelope (CLE). Biochim Biophys Acta 2014:314–318
7. Natsuga K (2014) Epidermal barriers. Cold Spring Harb Perspect Med 4:a018218–a018218
8. Tsuruta D, Green KJ, Getsios S, Jones JCR (2002) The barrier function of skin: how to keep a tight lid on water loss. Trends Cell Biol 12:355–357 [PubMed: 12191905]
9. Kobayashi T, Naik S, Nagao K (2019) Choreographing immunity in the skin epithelial barrier. Immunity 50:552–565 [PubMed: 30893586]
10. Fu M, Blackshear PJ (2017) RNA-binding proteins in immune regulation: a focus on CCCH zinc finger proteins. Nat Rev Immunol 17:130–143 [PubMed: 27990022]
11. Uehata T, Akira S (1829) mRNA degradation by the endoribonuclease Regnase-1/ZC3H12a/MCPIP-1. Biochim Biophys Acta 2013:708–713
12. Iwasaki H, Takeuchi O, Teraguchi S, Matsushita K, Uehata T, Kuniyoshi K, Satoh T, Saitoh T, Matsushita M, Standley DM et al. (2011) The IkappaB kinase complex regulates the stability of

cytokine-encoding mRNA induced by TLR-IL-1R by controlling degradation of regnase-1. Nat Immunol 12:1167–1175 [PubMed: 22037600]

13. Uehata T, Iwasaki H, Vandenbon A, Matsushita K, Hernandez-Cuellar E, Kuniyoshi K, Satoh T, Mino T, Suzuki Y, Standley DM et al. (2013) Malt1-induced cleavage of Regnase-1 in CD4(+) helper T cells regulates immune activation. Cell. 153:1036–1049 [PubMed: 23706741]
14. Li M, Cao W, Liu H, Zhang W, Liu X, Cai Z, Guo J, Wang X, Hui Z, Zhang H et al. (2012) MCPIP1 down-regulates IL-2 expression through an ARE-independent pathway. PLoS One 7:e49841
15. Mizgalska D, Wegrzyn P, Murzyn K, Kasza A,Koj A,Jura J, Jarzab B, Jura J (2009) Interleukin-1-inducible MCPIP protein has structural and functional properties of RNase and participates in degradation of IL-1beta mRNA. FEBS J 276:7386–7399 [PubMed: 19909337]
16. Monin L, Gudjonsson JE, Childs EE, Amatya N, Xing X, Verma AH, Coleman BM, Garg AV, Killeen M, Mathers A et al. (2017) MCPIP1/Regnase-1 restricts IL-17A- and IL-17C-dependent skin inflammation. J Immunol 198:767–775 [PubMed: 27920272]
17. Ruiz-Romeu E, Ferran M, Gimenez-Arnau A, Bugara B, Lipert B, Jura J, Florencia EF, Prens EP, Celada A, Pujol RM et al. (2016) MCPIP1 RNase is aberrantly distributed in psoriatic epidermis and rapidly induced by IL-17A. J Invest Dermatol 136:1599–1607 [PubMed: 27180111]
18. Takaishi M, Satoh T, Akira S, Sano S (2018) Regnase-1, an immunomodulator, limits the IL-36/IL-36R autostimulatory loop in keratinocytes to suppress skin inflammation. J Invest Dermatol 138:1439–1442 [PubMed: 29339122]
19. Jeltsch KM, Hu D, Brenner S, Zoller J, Heinz GA, Nagel D, Vogel KU, Rehage N, Warth SC, Edelmann SL et al. (2014) Cleavage of Roquin and Regnase-1 by the paracaspase MALT1 releases their cooperatively repressed targets to promote T(H)17 differentiation. Nat Immunol 15:1079–1089 [PubMed: 25282160]
20. Jura J, Skalniak L, Koj A (1823) Monocyte chemotactic protein-1induced protein-1 (MCPIP1) is a novel multifunctional modulator of inflammatory reactions. Biochim Biophys Acta 2012:1905–1913
21. Matsushita K, Takeuchi O, Standley DM, Kumagai Y, Kawagoe T, Miyake T, Satoh T, Kato H, Tsujimura T, Nakamura H et al. (2009) Zc3h12a is anRNase essential for controlling immune responses by regulating mRNA decay. Nature. 458:1185–1190 [PubMed: 19322177]
22. Zhou Z, Miao R, Huang S, Elder B, Quinn T, Papasian CJ, Zhang J, Fan D, Chen YE, Fu M (2013) MCPIP1 deficiency in mice results in severe anemia related to autoimmune mechanisms. PLoS One 8: e82542
23. Liang J, Saad Y, Lei T, Wang J, Qi D, Yang Q, Kolattukudy PE, Fu M (2010) MCP-induced protein 1 deubiquitinates TRAF proteins and negatively regulates JNK and NF-kappaB signaling. J Exp Med 207:2959–2973 [PubMed: 21115689]
24. Miao R, Huang S, Zhou Z, Quinn T, Van Treeck B, Nayyar T, Dim D, Jiang Z, Papasian CJ, Eugene Chen Y et al. (2013) Targeted disruption of MCPIP1/Zc3h12a results in fatal inflammatory disease. Immunol Cell Biol 91:368–376 [PubMed: 23567898]
25. Swindell WR, Sarkar MK, Liang Y, Xing X, Gudjonsson JE (2016) Cross-disease transcriptomics: unique IL-17A signaling in psoriasis lesions and an autoimmune PBMC signature. J Invest Dermatol 136:1820–1830 [PubMed: 27206706]
26. Li Y, Huang X, Huang S, He H, Lei T, Saaoud F, Yu XQ, Melnick A, Kumar A, Papasian CJ et al. (2017) Central role of myeloid MCPIP1 in protecting against LPS-induced inflammation and lung injury. Signal Transduct Target Ther 2:17066 [PubMed: 29263935]
27. Hafner M, Wenk J, Nenci A, Pasparakis M, Scharffetter-Kochanek K,Smyth N, Peters T, Kess D,Holtkotter O, Shephard P et al. (2004) Keratin 14Cre transgenic miceauthenticate keratin14as an oocyteexpressed protein. Genesis 38:176–181 [PubMed: 15083518]
28. Anders S, Pyl PT, Huber W (2015) HTSeq—a Python framework to work with high-throughput sequencing data. Bioinformatics. 31: 166–169 [PubMed: 25260700]
29. Huang DW, Sherman BT, Lempicki RA (2009) Systematic and integrative analysis of large gene lists using DAVID bioinformatics resources. Nat Protoc 4:44–57 [PubMed: 19131956]

30. Huang DW, Sherman BT, Lempicki RA (2009) Bioinformatics enrichment tools: paths toward the comprehensive functional analysis of large gene lists. Nucleic Acids Res 37:1–13 [PubMed: 19033363]
31. Hardman MJ, Sisi P, Banbury DN, Byrne C (1998) Patterned acquisitionofskinbarrier functionduring development. Development 125:1541–1552 [PubMed: 9502735]
32. Heyden A, Lutzow-Holm C, Clausen OP, Brandtzaeg P, Huitfeldt HS (1994) Expression of keratins K6 and K16 in regenerating mouse epidermis is less restricted by cell replication than the expression of K1 and K10. Epithelial Cell Biol 3:96–101 [PubMed: 7534576]
33. Stoler A, Kopan R, Duvic M, Fuchs E (1988) Use of monospecific antisera and cRNA probes to localize the major changes in keratin expression during normal and abnormal epidermal differentiation. J Cell Biol 107:427–446 [PubMed: 2458356]
34. Mils V, Vincent C, Croute F, Serre G (1992) The expression of desmosomal and corneodesmosomal antigens shows specific variations during the terminal differentiation of epidermis and hair follicle epithelia. J Histochem Cytochem 40:1329–1337 [PubMed: 1506670]
35. Coulombe PA (1997) Towards a molecular definition of keratinocyte activation after acute injury to stratified epithelia. Biochem Biophys Res Commun 236:231–238 [PubMed: 9240415]
36. McGowan K, Coulombe PA (1998) The wound repair-associated keratins 6, 16, and 17. Insights into the role of intermediate filaments in specifying keratinocyte cytoarchitecture. Subcell Biochem 31:173–204 [PubMed: 9932493]
37. Liew FY, Girard J-P, Turnquist HR (2016) Interleukin-33 in health and disease. Nat Rev Immunol 16:676–689 [PubMed: 27640624]
38. Vrotsos EG, Kolattukudy PE, Sugaya K (2009) MCP-1 involvement in glial differentiation of neuroprogenitor cells through APP signaling. Brain Res Bull 79:97–103 [PubMed: 19185603]
39. Niu J, Azfer A, Zhelyabovska O, Fatma S, Kolattukudy PE (2008) Monocyte chemotactic protein (MCP)-1 promotes angiogenesis via a novel transcription factor, MCP-1-induced protein (MCPIP). J Biol Chem 283:14542–14551 [PubMed: 18364357]
40. Chao J, Dai X, Pena T, Doyle DA, Guenther TM, Carlson MA (2015) MCPIP1 regulates fibroblast migration in 3-D collagen matrices downstream of MAP kinases and NF-kappaB. J Invest Dermatol 135:2944–2954 [PubMed: 26399696]
41. Lipert B, Wegrzyn P, Sell H, Eckel J, Winiarski M, Budzynski A, Matlok M, Kotlinowski J, Ramage L, Malecki M et al. (1843) Monocyte chemoattractant protein-induced protein 1 impairs adipogenesis in 3T3-L1 cells. Biochim Biophys Acta 2014:780–788
42. Zhussupbekova S, Sinha R, Kuo P, Lambert PF, Frazer IH, Tuong ZK (2016) A mouse model of hyperproliferative human epithelium validated by keratin profiling shows an aberrant cytoskeletal response to injury. EBioMedicine. 9:314–323 [PubMed: 27333029]
43. Garg AV, Amatya N, Chen K, Cruz JA, Grover P, Whibley N, Conti HR, Hernandez Mir G, Sirakova T, Childs EC et al. (2015) MCPIP1 endoribonuclease activity negatively regulates interleukin-17-mediated signaling and inflammation. Immunity. 43:475–487 [PubMed: 26320658]
44. Schafer M, Farwanah H, Willrodt A-H, Huebner AJ, Sandhoff K, Roop D, Hohl D, Bloch W, Werner S (2012) Nrf2 links epidermal barrier function with antioxidant defense. EMBO Mol Med 4:364–379 [PubMed: 22383093]
45. Haines RL, Lane EB (2012) Keratins and disease at a glance. J Cell Sci 125:3923 [PubMed: 23104737]
46. Lessard JC, Piña-Paz S, Rotty JD, Hickerson RP, Kaspar RL, Balmain A, Coulombe PA (2013) Keratin 16 regulates innate immunity in response to epidermal barrier breach. Proc Natl Acad Sci U S A 110:19537–19542 [PubMed: 24218583]
47. Helenius TO, Antman CA, Asghar MN, Nystrom JH, Toivola DM (2016) Keratins are altered in intestinal disease-related stress responses. Cells. 5. 10.3390/cells5030035
48. Di Salvo E, Ventura-Spagnolo E, Casciaro M, Navarra M, Gangemi S (2018) IL-33/IL-31 axis: a potential inflammatory pathway. Mediat Inflamm 2018:3858032
49. Kotsiou OS, Gourgoulianis KI, Zarogiannis SG (2018) IL-33/ST2 axis in organ fibrosis. Front Immunol 9:2432 [PubMed: 30405626]

50. Pinto SM, Subbannayya Y, Rex DAB, Raju R, Chatterjee O, Advani J, Radhakrishnan A, Keshava Prasad TS, Wani MR, Pandey A (2018) A network map of IL-33 signaling pathway. J Cell Commun Signal 12:615–624 [PubMed: 29705949]

51. Campbell L, Saville CR, Murray PJ, Cruickshank SM, Hardman MJ (2013) Local arginase 1 activity is required for cutaneous wound healing. J Invest Dermatol 133:2461–2470 [PubMed: 23552798]

52. Wynn TA, Vannella KM (2016) Macrophages in tissue repair, regeneration, and fibrosis. Immunity. 44:450–462 [PubMed: 26982353]

53. Watanabe M, Natsuga K, Nishie W, Kobayashi Y, Donati G, Suzuki S, Fujimura Y, Tsukiyama T, Ujiie H, Shinkuma S et al. (2017) Type XVII collagen coordinates proliferation in the interfollicular epidermis. eLife. 6. 10.7554/eLife.26635

54. Jackow J, Schlosser A, Sormunen R, Nystrom A, Sitaru C, Tasanen K, Bruckner-Tuderman L, Franzke C-W (2016) Generation of a functional non-shedding collagen XVII mouse model: relevance of collagen XVII shedding in wound healing. J Invest Dermatol 136:516–525 [PubMed: 26967482]

55. Hirako Y, Usukura J, Uematsu J, Hashimoto T, Kitajima Y, Owaribe K (1998) Cleavage of BP180, a 180-kDa bullous pemphigoid antigen, yields a 120-kDa collagenous extracellular polypeptide. J Biol Chem 273:9711–9717 [PubMed: 9545306]

56. Nishie W (2014) Update on the pathogenesis of bullous pemphigoid: an autoantibody-mediated blistering disease targeting collagen XVII. J Dermatol Sci 73:179–186 [PubMed: 24434029]

57. Schmitz J, Owyang A, Oldham E, Song Y, Murphy E, McClanahan TK, Zurawski G, Moshrefi M, Qin J, Li X et al. (2005) IL-33, an interleukin-1-like cytokine that signals via the IL-1 receptor-related protein ST2 and induces T helper type 2-associated cytokines. Immunity. 23:479–490 [PubMed: 16286016]

58. Talabot-Ayer D, Martin P, Vesin C, Seemayer CA, Vigne S, Gabay C, Palmer G (2015) Severe neutrophil-dominated inflammation and enhanced myelopoiesis in IL-33-overexpressingCMV/IL33 mice.J Immunol 194:750–760 [PubMed: 25505285]

59. Peng H, Ning H, Wang Q, Lu W, Chang Y, Wang TT, Lai J, Kolattukudy PE, Hou R, Hoft DF et al. (2018) Monocyte chemotactic protein-induced protein 1 controls allergic airway inflammation by suppressing IL-5-producing TH2 cells through the Notch/ Gata3 pathway. J Allergy Clin Immunol 142:582–594.e10

Key messages

- Loss of murine epidermal Mcpip1 upregulates transcripts related to inflammation and keratinocyte differentiation.
- Keratinocyte Mcpip1 function is essential to maintain the integrity of skin in adult mice.
- Ablation of Mcpip1 in mouse epidermis leads to the development of local and systemic inflammation.

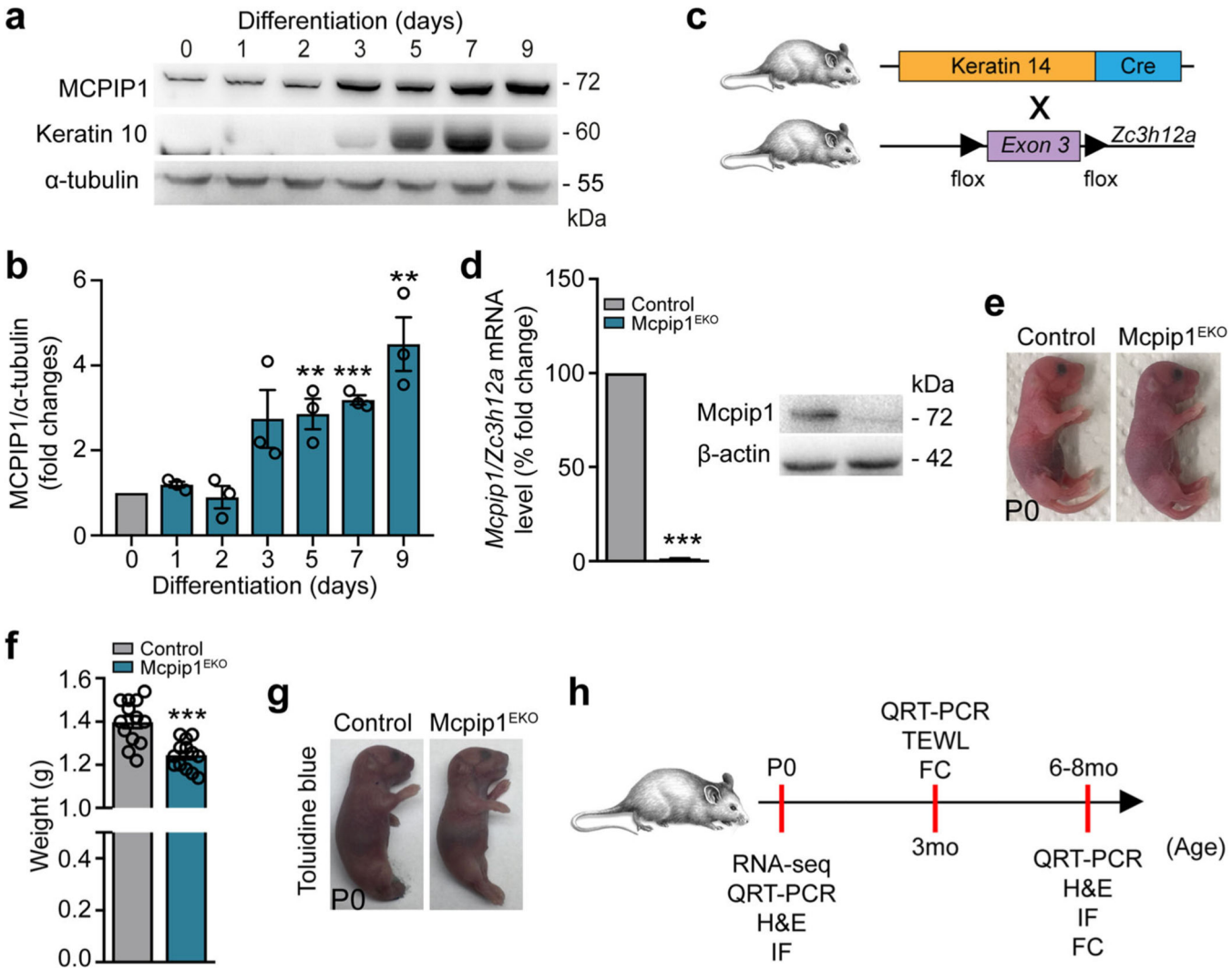

Fig. 1.

Conditional targeting of Mcpip1 in the epidermis. **a** Representative Western blot of three independent experiments for MCPIP1, keratin 10, and α-tubulin in primary human keratinocytes during Ca^{2+}-induced differentiation. **b** Densitometric quantification of MCPIP1 levels ($n = 3$). **c** The generation of conditional $Mcpip1^{EKO}$ mice [26, 27]. **d** Left: QRT-PCR analysis of *Mcpip1*/*Zc3h12a* transcript levels ($n = 7$); right: Western blot for Mcpip1 and β-actin in isolated mouse keratinocytes. **e** Macroscopic appearance of newborn (P0) pups. **f** Body weights of newborn (P0) pups ($n = 13$). **g** Toluidine blue dye penetration assay at P0. **h** Schematic diagram representing the time points for RNA-Seq, QRT-PCR, H&E, immunofluorescence (IF), TEWL, and FC analyses. Data represent the mean ± SEM. $^{**}P < 0.01$, $^{***}P < 0.001$ by unpaired *t* test

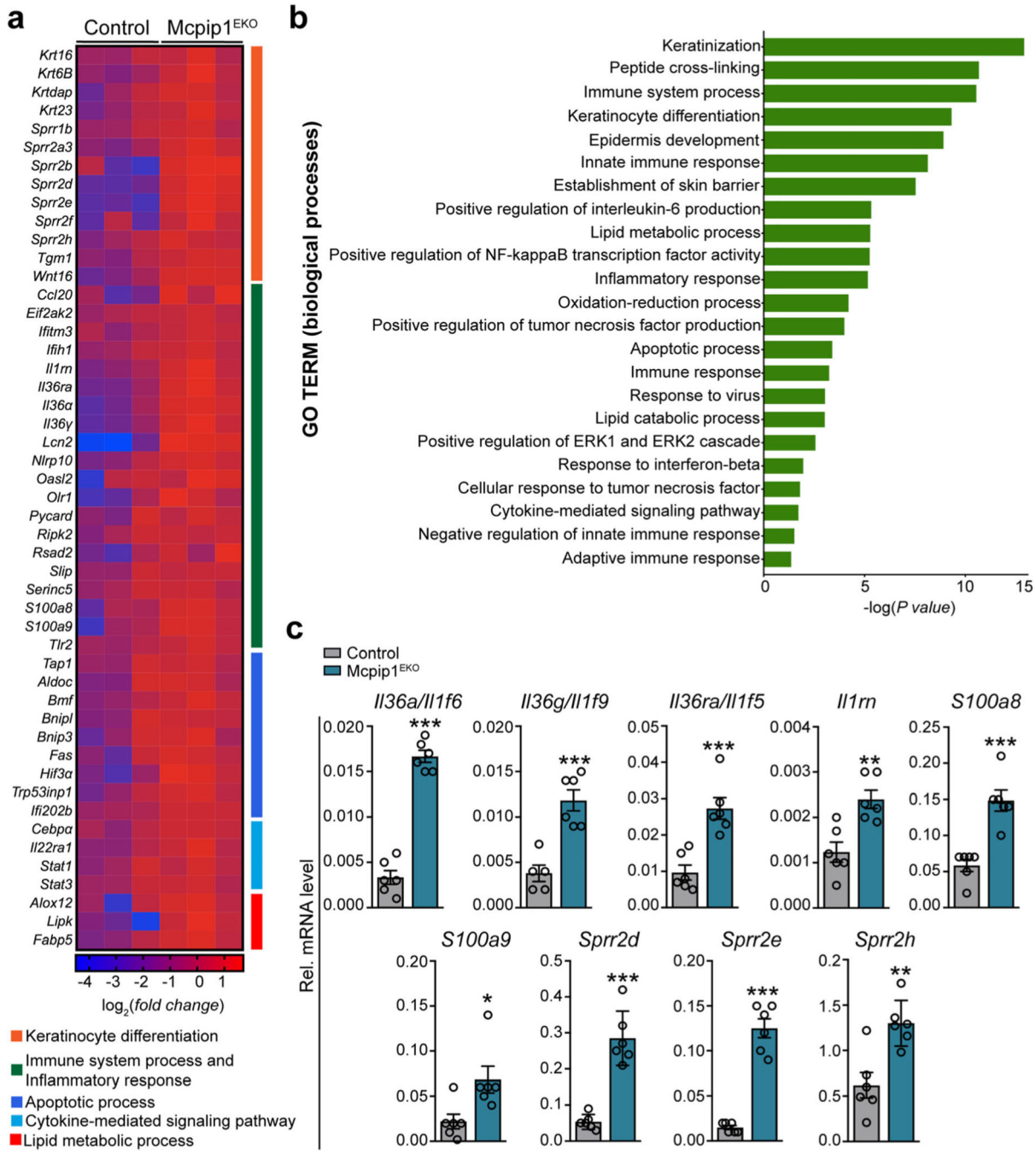

Fig. 2.

Epidermal Mcpip1 regulates the expression of genes involved in keratinocyte differentiation and the positive regulation of the immune response. RNA-Seq was performed on keratinocytes isolated from newborn Mcpip1^{EKO} or control mice ($n = 3$). **a** Heatmap expression plot of select genes. **b** GO biological process terms enriched among genes with upregulated expression in Mcpip1^{EKO} (adj. P value < 0.05 and fold change > 1.5). **c** QRT-PCR analysis of *Il36a/Il1f6, Il36g/Il1f9, Il36ra/ Il1f5, Il1rn, S100a8, S100a9, Sprr2d,*

Sprr2e, and *Sprr2h* expression ($n = 6$). Data represent the mean ± SEM. *$P < 0.05$, **$P < 0.01$, ***$P < 0.001$ by unpaired t test

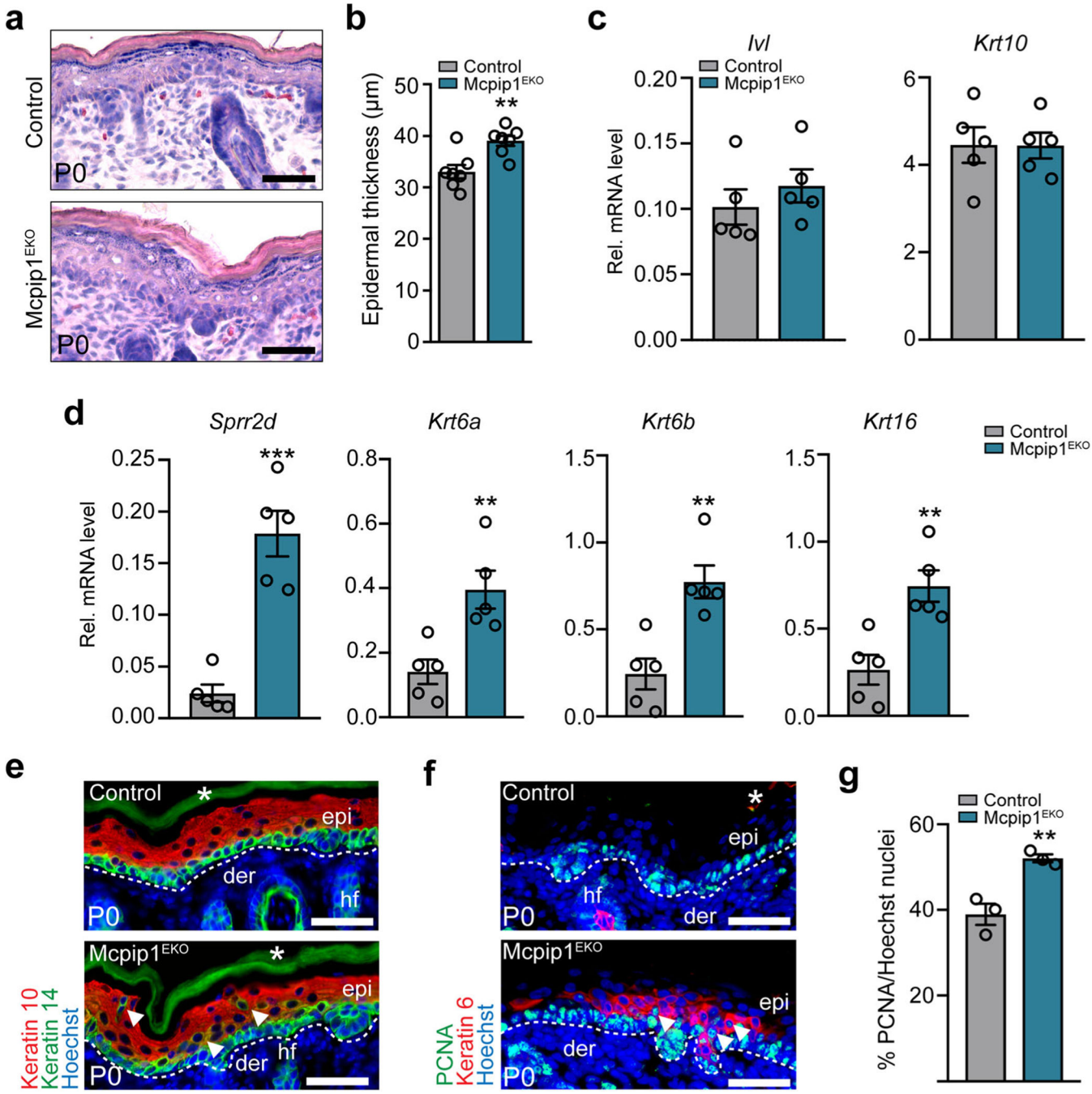

Fig. 3.

Newborn Mcpip1^{EKO} mice exhibit disturbances in the expression of epidermal proliferation and differentiation markers. **a** H&E-stained back skin at P0. **b** Quantification of the epidermal thickness at P0 ($n = 7$). **c** QRT-PCR analysis of *Ivl* and *Krt10* expression at P0 ($n = 5$). **d** QRT-PCR analysis of *Sprr2d*, *Krt6a*, *Krt6b*, and *Krt16* expression at P0($n = 5$). **e** Keratin 10 (Krt10) and keratin 14 (Krt14); **f** PCNA and keratin 6 immunofluorescence staining at P0. **g** Quantification of the epidermal PCNA-positive cells ($n = 3$). Arrowheads indicate Krt10/Krt14 double-positive suprabasal cells. Data represent the mean ± SEM. epi,

epidermis; der, dermis; hf, hair follicles; *, nonspecific signal. The dashed line indicates the basal membrane. Scale bar, 100 μm. ** $P < 0.01$, *** $P < 0.001$ by unpaired t test

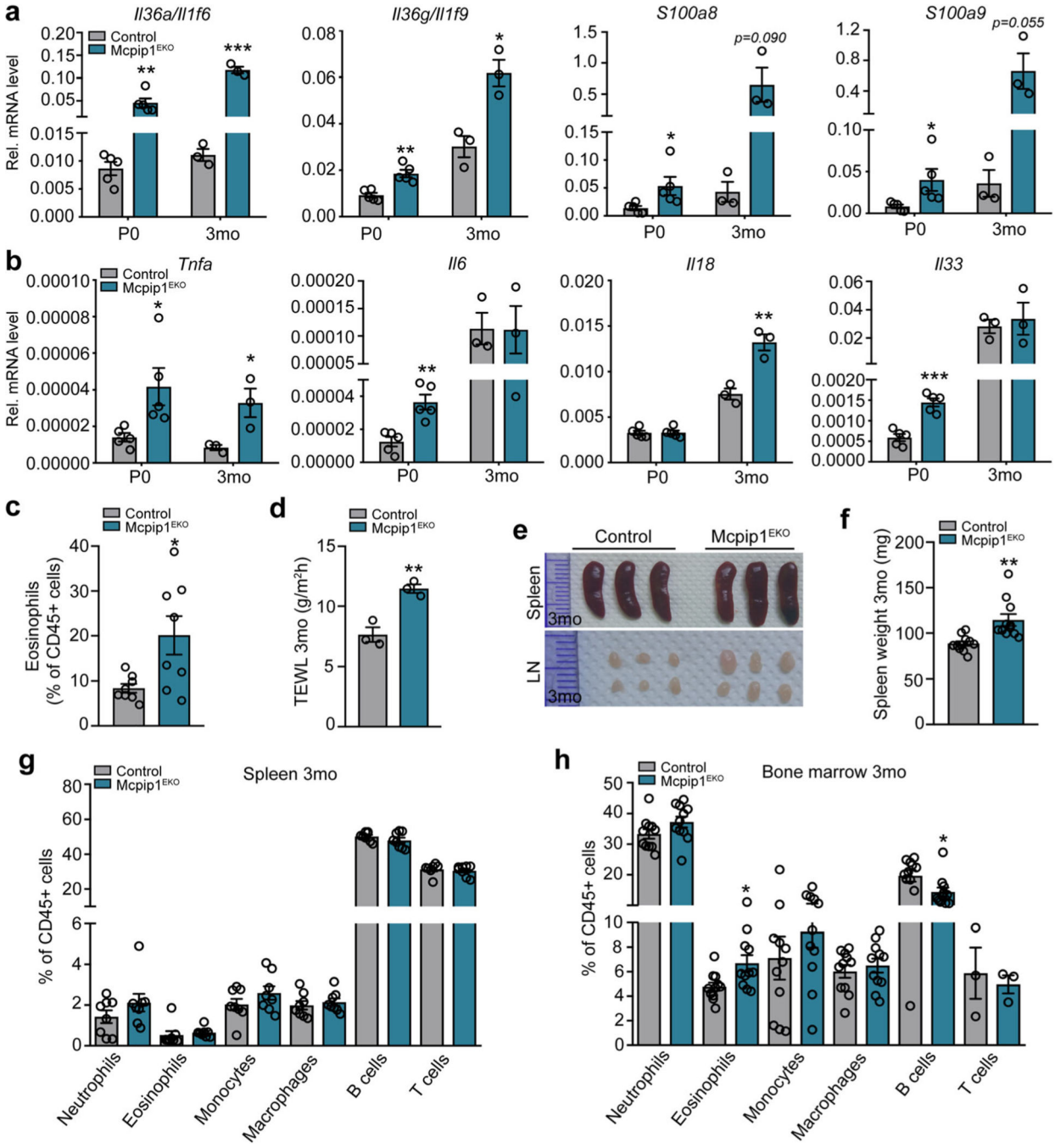

Fig. 4.

Newborn and young Mcpip1^{EKO} mice have elevated levels of inflammatory factors in their skin and develop mild systemic inflammation. QRT-PCR analysis of selected transcript levels in the control and Mcpip1^{EKO} newborn (P0, $n = 5$) and young (3 mo, $n = 3$) mice. **a** *Il36a/Il1f6, Il36g/Il1f9, S100a8, S100a9* transcript levels. **b** *Tnfa, Il6, Il18, and Il33* transcript levels. **c** Flow cytometric analysis of 3-monthold skin eosinophils ($n = 8$). **d** Quantification of TEWL in 3-month-old mice ($n = 3$). **e** Spleenandlymph node images of 3-month-old controland Mcpip1^{EKO} mice. **f** Spleen weights of 3-month-old control and

Mcpip1^{EKO} mice (n = 10). **g** Flow cytometric analysis of 3-month-old mouse splenic CD45+ cells (n = 8). **h** Flow cytometric analysis of 3-month-old mouse bone marrow CD45+ cells (n = 3–11). Data represent the mean ± SEM. *P < 0.05, **P < 0.01, ***P < 0.001 by unpaired t test

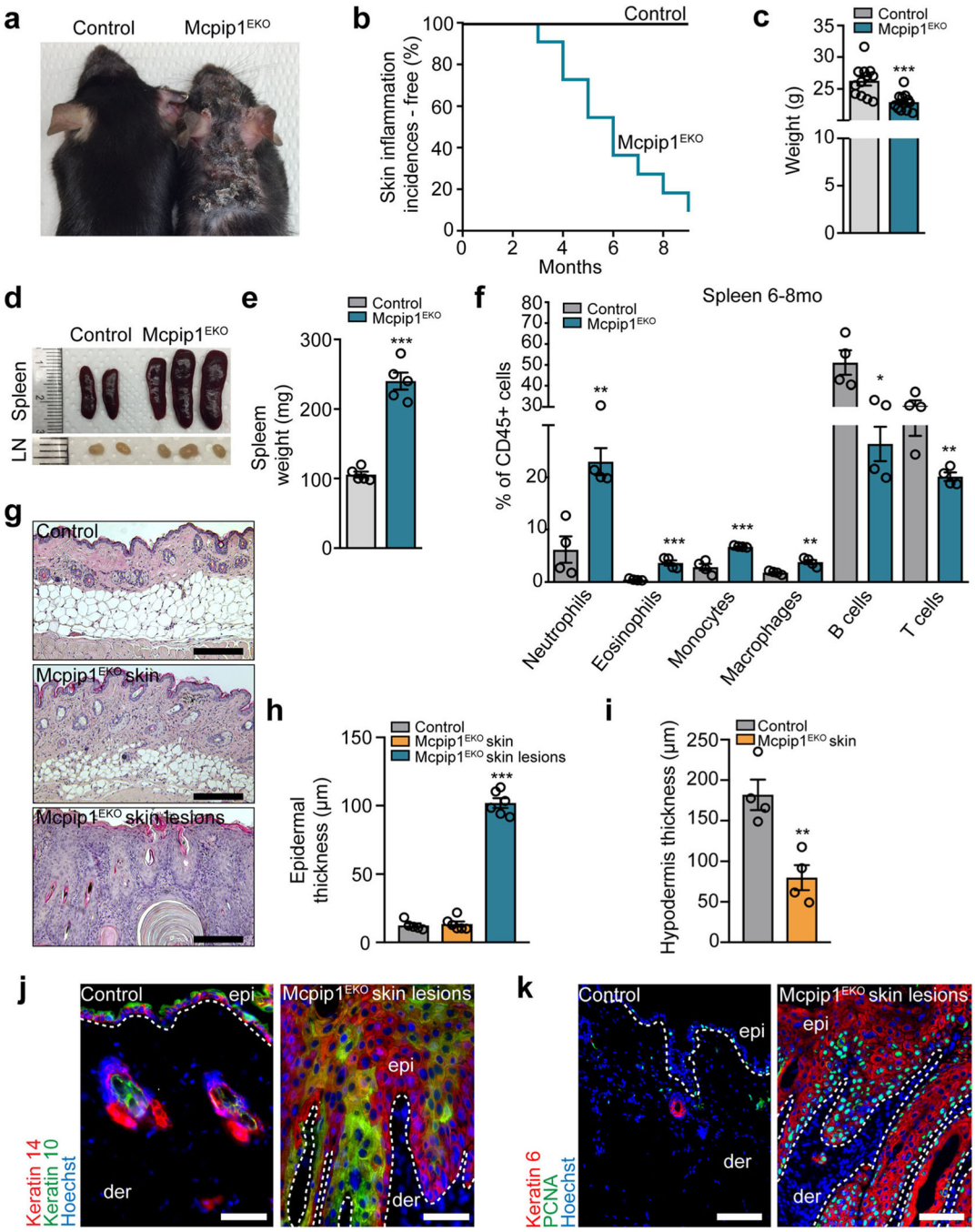

Fig. 5.

Development of skin lesions and systemic inflammation in old Mcpip1^{EKO} mice. **a** Macroscopic appearance of 6-month-old mice. **b** Kaplan-Meier plots for skin inflammation incidences ($n = 22$). **c** Body weights of 6- to 8-month-old mice ($n = 12$). **d** Spleen and lymph node images of 6-month-old mice. **e** Spleen weights of 6- to 8-month-old mice ($n = 5$). **f** Flow cytometric analysis of 6- to 8-month-old mouse splenic CD45+ cells ($n = 4$). **g** H&E staining of control and unaffected Mcpip1^{EKO} back skin and Mcpip1^{EKO} skin lesions. **h** Quantification of the epidermal thickness ($n = 6$). Mcpip1^{EKO} lesional skin was compared to

control skin. **i** Quantification of hypodermis in 6-month-old mice ($n = 4$). **j** Keratin 14 and keratin 10; **k** PCNA and keratin 6 immunofluorescence staining. Data represent the mean ± SEM; epi, epidermis; der, dermis. The dashed line indicates the basal membrane. Scale bar, 100 μm. *$P < 0.05$, **$P < 0.01$, ***$P < 0.001$ by unpaired *t* test or one-way ANOVA

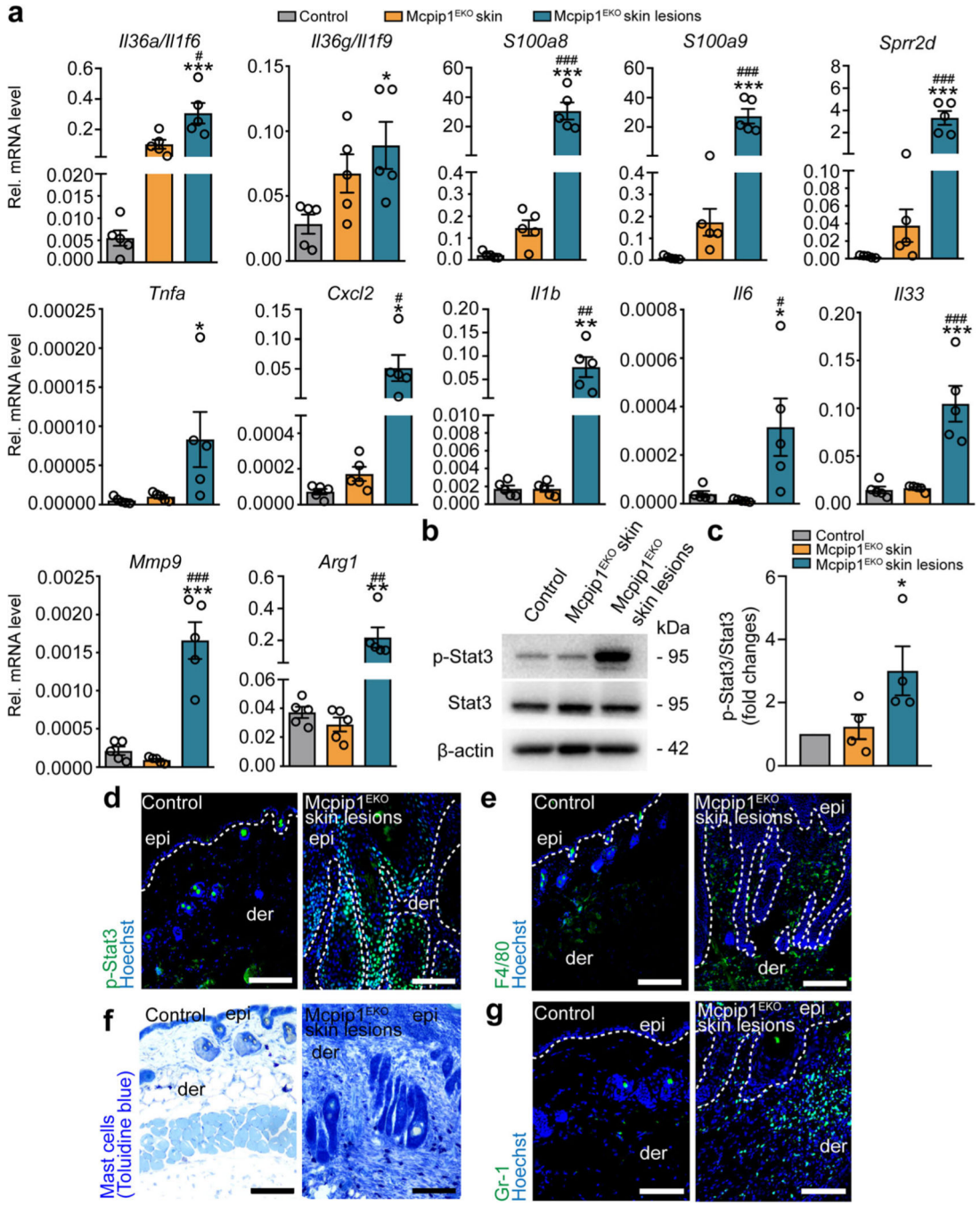

Fig. 6.

Old Mcpip1^{EKO} mice spontaneously develop skin inflammation. **a** QRT-PCR analysis of *Il36a/Il1f6, Il36g/Il1f9, S100a8, S100a9, Sprr2d, Tnfa, Cxcl2, Il1b, Il6, Il33, Mmp9*, and *Arg1* transcript levels in the healthy skin of the control and Mcpip1^{EKO} mice (6–8 mo) and in the skin lesions of Mcpip1^{EKO} mice ($n = 5$). **b** Representative Western blot for p-Stat3, Stat3, and β-actin in the control and Mcpip1^{EKO} mice (6–8 mo) from four independent experiments. **c** Densitometric quantification of p-Stat3/Stat3 levels ($n = 4$). **d** P-Stat3 immunofluorescence staining of the skin sections. **e** F4/80 immunostaining. **f** Toluidine

blue immunostaining. **g** Gr-1 immunostaining. Scale bar, 100 μm. Data represent the mean ± SEM; epi, epidermis; der, dermis. The dashed line indicates the basal membrane. $*P < 0.05$, $**P < 0.01$, $***P < 0.001$ by one-way ANOVA. * refers to the comparison of control and Mcpip1^{EKO} skin lesions; # refers to the comparison of Mcpip1^{EKO} skin and Mcpip1^{EKO} skin lesions